Available online at www.sciencedirect.com
SCIENCE DIRECT®
Journal of Nuclear Materials 328 (2004) 124–136
journal of nuclear materials
www.elsevier.com/locate/jnucmat

Surface chemistry of Pu oxides

J. Douglas Farr *, Roland K. Schulze, Mary P. Neu

Los Alamos National Laboratory, MS G721, P.O. Box 1663, Los Alamos, NM 87455, USA

Received 16 December 2003; accepted 15 March 2004

Abstract

X-ray photoelectron spectroscopy was used to examine the surface chemistry of a variety of Pu(IV) compounds, including PuO_2 and $Pu(OH)_4$. The Pu 4f, O 1s and C 1s binding energy regions were line shape fit to unequivocally demonstrate that multiple species are present. Surface hydroxyls were ubiquitous in all PuO_2 samples exposed to H_2O vapor or ambient air, and persisted with heating to 590 °C. Active surface sites for the reaction of H_2O and other small molecules and spectral features consistent with pure stoichiometric PuO_2 can be regenerated by thermal energy or by effects of a radiation field. Evidence of higher valence Pu species was observed in some treated samples with the formula PuO_{2+x}.
Published by Elsevier B.V.

1. Introduction

It has been suggested that surface reactions between plutonium (Pu) oxide powders and water (H_2O) vapor could result in explosive conditions at Pu storage facilities and increased solubility and migration of environmental Pu contamination [1,2]. Pu metal in excess of national defense needs and residues from decades of Pu processing are being stabilized for storage. Current US Department of Energy plans call for the storage of excess Pu by converting it to the dioxide and placing it in sealed steel containers [3,4]. Reactions at the interface between solid Pu oxide particles, adsorbed materials and the vapor phase play a dominant role in determining the resultant surrounding atmosphere and stability of the solids. Understanding the chemistry at this interface, particularly with respect to reactions with H_2O vapor, is crucial for predicting the storage behavior of these powders. Safe storage of Pu oxide requires minimal exposure to H_2O vapor in order to limit chemically or radiolytically driven gas generation reactions. It may also depend on limiting container storage time and container corrosion rates.

Surface reactions and the resultant products are also important to the fate of environmental Pu contamination. For example, surfacial Pu(V) or Pu(VI) species may be expected to increase Pu solubility in groundwaters and subsurface environments and thereby increase Pu migration rates from past processing and waste facilities onto public lands [5]. Reactions at the solid–water interface are important for understanding Pu adsorption and desorption from minerals and ceramics.

This work investigates the chemical nature of the surfaces of plutonium dioxide (PuO_2), Pu hydroxide and hyperstoichiometric Pu oxide powders. X-ray photoelectron spectroscopy (XPS) provides reliable reference spectra for the Pu 4f and O 1s levels of pure materials that can be applied to more complex systems. Binding energies for Pu metal, Pu_2O_3 and PuO_2 are fairly well established [6–9], and some Pu halides and oxyhalides have been studied [10,11]. Most of studies were of pure materials that are free of surface H_2O and H_2O reaction products and as free as possible from other common contaminants such as C that are present on surfaces exposed to the atmosphere. The binding energy values,

* Corresponding author: Tel.: +1-505 667 4033; fax: +1-505 667 1058.
E-mail address: d.farr@lanl.gov (J.D. Farr).

0022-3115/$ - see front matter Published by Elsevier B.V.
doi:10.1016/j.jnucmat.2004.04.001

distinctive line shapes, and peak widths that have been obtained in previous work on well-characterized material are used to interpret measured spectra of more complex oxides, mineral-adsorbed species, and unknown forensic samples.

2. Experimental

One of the difficulties of working with Pu materials is their chemical and radiotoxicity, which precludes unrestricted studies. The work described here was completed in dedicated laboratories with appropriate engineered controls and extensive air and personnel monitoring. X-ray photoelectron spectroscopy (XPS) was used to investigate the surface chemistry of a variety of samples of Pu oxides, hydroxides and a carbonate. The apparatus used for most of these measurements was a Kratos XSAM 800 X-ray photoelectron spectrometer system. High-resolution spectra were acquired at 20 eV pass energy using Mg Kα X-rays and an acceptance half-angle of 25°. No flood gun charge compensation was used in these measurements. Charge correction was performed by referencing the adventitious (hydrocarbon-like) C to 284.6 eV binding energy. Thermal dehydration treatments were performed while maintaining a base pressure of 2×10^{-9} Torr. Data was collected after at least 30 min equilibration at chosen temperatures. The XPS data were also collected in earlier experiments using a Physical Electronics (PHI) 15-255G cylindrical mirror analyzer (CMA). Mg Kα X-rays were used to excite the samples and data was collected at a pass energy of 50 eV.

The PuO_2 starting material for some of the experiments was synthesized by the oxidation of doubly refined α Pu metal. The typical metallic impurities were on the order of 400 ppm. The metal was fired in air at 1000 °C, resulting in oxide powders with an average particle size of about 10 μm. These 'high-fired' Pu oxide powder samples were studied in the as-received (atmospheric exposure condition), in heating (dehydration) experiments up to 590 °C, exposed to air after dehydration, and after controlled exposures to H_2O vapor.

Plutonium(IV) hydroxide solid, colloidal Pu(IV) hydroxides, and Pu(VI) carbonate were prepared from weapons grade Pu metal or oxide (approximately 94% by weight ^{239}Pu and 6% ^{240}Pu). Stock solutions were prepared by dissolving the solids in 4 M $HClO_4$ or other mineral acids and assayed for Pu(IV) concentration and oxidation state purity using optical absorbance spectroscopy.

Plutonium(IV) hydroxide was prepared by diluting a 1.0 mL aliquot of a 0.63 M Pu stock solution into 5.0 mL of distilled, deionized H_2O. The pH of that solution was raised to 10.2 using 5.0 and 1.0 M NaOH. The resulting green precipitate was washed three times with distilled, deionized H_2O, then washed with acetone (CH_3COCH_3) and dried in air. Hydroxide powders prepared in this manner are reportedly distinct from the colloidal materials that can be prepared by treating Pu solutions with weaker bases or peptizing the solid hydroxide [12].

Colloidal Pu(IV) hydroxide was prepared using the method reported by Lloyd and Haire [13] as follows: a Pu(IV) stock solution was prepared by dissolving weapons grade Pu (approximately 94% by weight ^{239}Pu and 6% ^{240}Pu) in 4 M $HClO_4$ and assayed for Pu(IV) using optical absorbance spectroscopy. A 0.52 mL aliquot of the resulting 0.76 M Pu stock solution was added to 3.0 mL of 4.0 M HNO_3. The pH of the resultant solution was raised to 6 using concentrated NH_4OH and then to 9.15 using 25% NH_4OH to yield a finely divided, green precipitate. The solid was washed with distilled, deionized H_2O six times and peptized in 0.08 M HNO_3. After heating at 82 °C for 8 h and adding 0.5 mL of 8 M HNO_3, approximately 75% of the material was suspended in solution. The suspension was then placed in a sonicator for 60 min The final solution concentration was determined using previously established extinction coefficients for colloidal Pu(IV) hydroxide formed under similar conditions. The final solution pH was 1.7. The suspension was centrifuged at 7000 rpm for 10 min to remove larger sized colloids. An aliquot from the top of the solution column was removed and dehydrated to produce the common, nitrate-based colloid sample referred to as Pu(IV) colloid n. Material prepared using this method reportedly has a particle size of approximately 2 nm and a NO_{3-} to Pu^{4+} ratio of approximately 0.80 [14].

A second colloidal Pu(IV) hydroxide was similarly prepared by Haire, et al., but heated and dried such that the nitrate concentrate is significantly reduced and the colloids aggregate. The final product was previously determined to have a size of ~80–100 Å and a NO_{3-} to Pu^{4+} ratio of approximately 0.1–0.15 [14]. This sample is referred to as Pu(IV) colloid a.

Plutonium(VI) carbonate, PuO_2CO_3, was prepared by adding 25% NH_4OH to a 0.5 M HNO_3, 0.1 M Pu(VI) stock solution of weapons grade Pu to pH 7 followed by bubbling CO_2 through the stirred solution for two days. The PuO_2CO_3 precipitated from the solution as a pink-brown solid which was washed twice with distilled, deionized H_2O. The solid was suspended in H_2O and CO_2 was bubbled through the stirred suspension for three to five days. Ozone was also bubbled through the suspension for the final two days to reoxidize any Pu that had reduced via radiolysis. The resulting pink-brown solid was characterized using powder X-ray diffraction (INEL CPS-120 powder X-ray diffractometer), extended X-ray absorbance fine structure (EXAFS) spectroscopy, and diffuse reflectance spectroscopy. All of these analyses

indicated that the material was isostructural with rutherfordine, UO_2CO_3 [15].

Hyperstoichiometric oxides, described elsewhere [5], are Pu oxide powders with the formula PuO_{2+x}. The samples analyzed in this study were formed by the reaction of high-fired PuO_2 with H_2O vapor at elevated temperatures. The calculated composition for the material used in this work is $PuO_{2.26}$, based on the pressure of H_2 generated during the reaction at 300 °C [16]. The slightly expanded cubic lattice parameter for this material was 0.54022 nm, compared to 0.53975 nm for stoichiometric PuO_2. The structure PuO_{2+x} remains unresolved; thus, the fraction of Pu existing at higher oxidation states in this material depends on how charges are balanced within various proposed model structures. One such structure [17], places a hydroxyl ion at the FCC body center, and requires the oxidation of a Pu(IV)—O to Pu(V)═O. The formula for this model would more correctly be Pu_4O_8OH, consisting of three Pu(IV) atoms and one Pu(V) atom. Other proposed models place an extra O atom in various positions in the FCC lattice, including in the central octahedral site. Some charge transfer from the existing Pu atoms must occur to balance the additional O, but the details are still unknown. For most of the material analyzed in this study, Pu is in the +4 oxidation state, with the exception of PuO_2CO_3, which is in the +6 oxidation state. The value for x in PuO_{2+x} could be as high as 0.27, depending on preparation conditions, implying the presence of Pu in higher oxidation states. Samples were usually mounted on conductive carbon (C) tape or, if thermal treatments were planned, pressed into gold (Au) foil.

The powders spanned a range of specific activities from 0.003 Ci/g (less than 0.1 mW/g) for a $^{242}PuO_2$ powder to a rather high specific activity of 7.4 Ci/g (12 mW/g) for ^{241}Pu-enriched $^{239}PuO_2$ powder. This high activity material was obtained during a forensic exercise that was designed to characterize unknown nuclear material. Although its origin is unknown, isotope concentration estimates obtained by mass spectroscopy for ^{238}Pu, ^{239}Pu, ^{240}Pu, ^{241}Pu and ^{242}Pu were 1.9%, 57.3%, 26.4%, 7.8%, and 6.6% mass percentages, respectively. Typical 'weapons grade' material is approximately 95% ^{239}Pu and much lower in ^{238}Pu and ^{241}Pu, with a specific activity of less than 1 Ci/g (less than 2 mW/g). Differences in specific activity had an apparent effect on surface chemistry for these material, with effects being roughly linear, that is, becoming more pronounced at higher activities. The primary decay mode for ^{242}Pu is by the emission of 5 MeV alpha particles, but the longer half-life of this isotope yields a much lower specific activity relative to the other samples. The high activity of the unknown material was largely due to the elevated ^{241}Pu content, which decays primarily by the emission of 20 keV beta particles. A more significant difference from the typical isotope mix, however, is due to an increase in ^{238}Pu content (compared to typical Pu oxide) by about three orders of magnitude. The 5 MeV alpha particles emitted by ^{238}Pu have the potential to deposit a great deal more energy at the surface than the beta particles. While the energy transfer of these decay products differ, both can affect adsorbate surface chemistry, depending on the specific activity due to varying isotope ratios. The particle flux at the surface is sufficient to desorb small molecules and/or break bonds with surface adsorbates, resulting in a 'cleaner' surface. Surface analysts use a technique called electron beam stimulated desorption (EBSD) that is based on the removal of surface species using incident electron energies of 5–20 eV. Typical bond strengths are only a few eV, easily broken by the energetic alpha and beta particles, as well as the secondary electrons that are produced. Hydroxide to oxide ratios for the low ($^{242}PuO_2$), medium (typical oxide) and high activity samples were about 20, 5 and 1, respectively. These values correlate well with the specific activities (and power/mass) of the samples and are a relative measure of surface layer thickness. The surface morphology and particle size distribution of the powders can differ according to processing conditions. It is recognized that these properties also affect surface chemistry, however a systematic study of these effects is beyond the scope of this study.

3. Results and discussion

3.1. Various Pu(IV) oxides

XPS has been used for many years to characterize oxidized Pu metal surfaces and Pu-containing materials. Pu 4f core levels are typically used to confirm the presence of Pu on surfaces and gather information about its chemical state. During the analysis of air-oxidized Pu metal, we have observed subtle shifts to higher binding energies and/or broadening of the Pu 4f peaks compared to standard PuO_2 spectra created by oxidizing clean metal under UHV. Pu deposited on surfaces from aqueous or vapor phases also show this broadening and binding energy increase. These spectra still contain the basic spectroscopic features associated with Pu(IV) oxide, but other chemical states appear to be present. In the past, most analysts dismissed these spectra as too complex to unravel or the result of charging problems. Often the only other elements detected are C and O, both in great abundance and in multiple chemical states. The following results show that one of the most abundant surface species on these air-exposed samples is Pu(IV) hydroxide.

The spectra presented and described here were obtained using the Kratos system and are consistent with earlier work on a variety of nominally Pu(IV) compounds that was done using a PHI 15-255G double pass

CMA. The PHI instrument has somewhat lower resolution than the Kratos system, but overall trends were consistent between both systems for all the data collected. Fig. 1 shows the Pu 4f and O 1s regions that were collected from a series of Pu (IV) oxide powders. The spectra were collected from standard high-fired PuO_2 powder, treated PuO_2 powder (PuO_{2+x}), $Pu(OH)_4$ and two different preparations of dried Pu(IV) colloid powder, shown from the top of the figure to the bottom, respectively.

The upper traces in Fig. 1 are from a high-fired PuO_2 powder. Pu 4f photoemission peaks show a spin–orbit doublet for the Pu $4f_{5/2}$ and Pu $4f_{7/2}$ peaks at about 439 eV and about 426 eV, where they have been previously reported [6]. Well-defined shake-up satellite peaks are seen about 6 eV above the main peaks for PuO_2. These are energy loss peaks that appear in Pu(IV) compounds [11]. The intensity of the shake-up satellites diminishes and the band width increases for the other materials, particularly for the colloidal Pu(IV). The O 1s region for PuO_2 shows greater intensity at lower binding energies than the other materials, indicating that more of the oxygen is bound to Pu as the dioxide at 529.5 eV. The intensity at higher binding energies is likely due to surface hydroxides, and matches well with the peak position seen in the O 1s region for $Pu(OH)_4$ (531.8 eV), described below. Pu 4f binding energies for the colloidal material are very similar to those observed for the hydroxide compound. This is not surprising, since colloidal Pu(IV) is thought to be composed of extended polymer-like hydroxylated Pu oxides, in which different O ligands will form different types of bonds with Pu [18–20]. Water may also be a component of this material and is consistent with the greater intensity observed at higher binding energies in the O 1s region. The trends in binding energy shifts are generally consistent with those reported for transition metal hydroxides and $Mg(OH)_2$ [21]. That is, shifts to higher binding energies are observed with the addition of hydroxyls or with adsorbed H_2O. The highest binding energy shifts observed in the Pu 4f region are for PuO_{2+x}, indicating that Pu is in a more electron-withdrawing environment here than in $Pu(OH)_4$. Under ideal conditions, the shake-up satellites can be used to quantify the amount of Pu(IV) present relative to the other oxidation states of Pu. An oxidation state pure Pu(IV) compound produces satellite peaks with intensities that are a certain fraction of the intensity of the main peaks. If the satellites are less intense with respect to the main peaks (than expected for an oxidation-state pure material) then oxidation state(s) other than +4 are present. Changes in the main peak to satellite ratios can be subtle, particularly when two or more Pu(IV) compounds that have slightly different binding energies are present. Because satellite peaks shift along with the main peaks, energy changes can be obscured. Shifts of the main Pu 4f peaks to higher binding

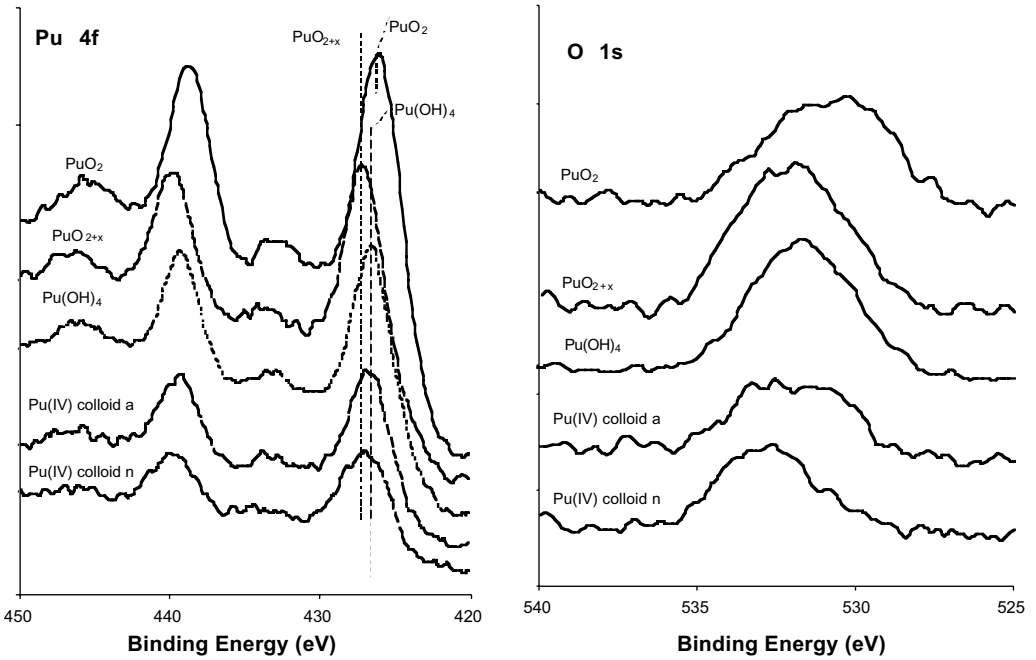

Fig. 1. Various Pu oxide preparations. Pu 4f and O 1s regions from a variety of Pu(IV) oxide preparations showing the range of binding energies observed for these materials. The subtle shifts and rather broad features suggest a variety of surface chemistries.

energies without any shifts or increased intensity in the satellite peaks, observed for PuO_{2+x}, suggest the presence of Pu oxidation states higher than +4.

3.2. Thermal treatments of PuO_2 powders

The complexities illustrated in Fig. 1 made it clear that there are a variety of surface chemical states possible for Pu(IV), and that a systematic study was needed to identify individual components. Thermal treatments were used to desorb H_2O and other labile surface species under ultra-high vacuum (UHV) conditions while collecting XPS data as the temperature was increased. After heating, one of the samples was exposed to H_2O vapor and another exposed to ambient air. XPS data from all of these experiments is discussed below.

3.3. $^{239}PuO_2$

A sample of the high-fired $^{239}PuO_2$ powder was exposed to high humidity. The oxide was placed in an open vial, which for two weeks was placed in a shallow, closed vessel that contained 3.4 M H_2SO_4, resulting in a relative humidity of 97.5%. The sample was then analyzed by XPS in the as-received condition, after heating to 100, 150, 200, 400, 590 °C and after exposure to 10^{10} L H_2O. The XPS data for the Pu $4f_{7/2}$ and O 1s core levels from the as-received condition through the thermal treatments up to 590 °C and subsequent exposure to H_2O vapor are shown in Fig. 2. The Pu 4f and O 1s peak widths narrow and decrease in binding energy as the surface loses hydroxides and oxy-carbon species at higher temperatures and becomes more like bulk PuO_2. The broad distribution of chemical states observed in Pu $4f_{7/2}$ for the as-received sample gradually loses intensity on the high binding energy side as heating progresses, resulting in a single peak for PuO_2 at 425.5 eV for the 400 °C treatment. Corresponding changes are also observed in the O 1s spectra through the heating regimes. Initially, the surface is dominated by hydroxide and hydroxide-like states represented by the broad peak at about 532 eV. The shoulder at 529.5 eV corresponding to lattice O increases in intensity relative to the higher binding energy peak as the temperature increases. By 200 °C the lattice oxide peak intensity is comparable to the hydroxide intensity, then dominates at higher temperatures. At 590 °C, the O 1s peak is primarily from PuO_2, but some rather tenacious surface hydroxyls persist. A shoulder of low intensity appears on the low binding energy side of the 590 °C Pu $4f_{7/2}$ peak at about

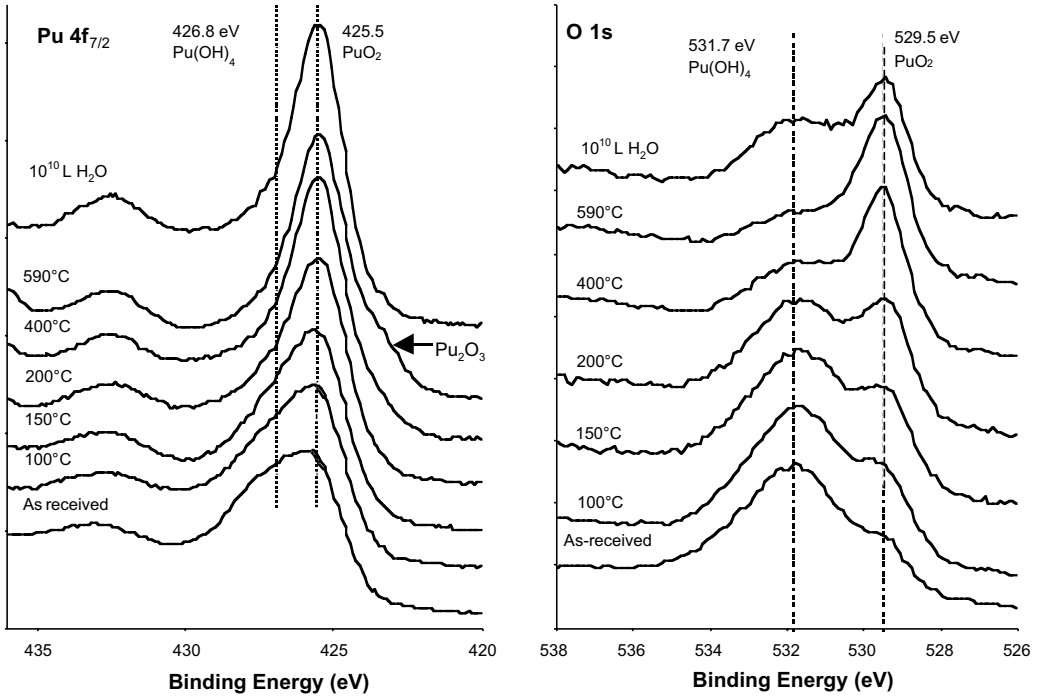

Fig. 2. $^{239}PuO_2$ thermal dehydration. Pu $4f_{7/2}$ and O 1s core levels for a $^{239}PuO_2$ powder in the as-received condition, through a series of thermal treatments, then followed by exposure to 10^{10} L H_2O. Pu 4f peaks narrow and become more bulk dioxide-like as the O 1s dioxide peak grows with respect to the hydroxide intensity. Exposure to H_2O vapor restores some surface hydroxides and eliminates the reduced Pu oxide.

424 eV, where Pu_2O_3 is expected, indicating some reduction of the surface PuO_2 under the influence of this temperature and ultra-high vacuum. After exposure to 10^{10} L H_2O, the Pu_2O_3 feature disappears and the hydroxyl peak grows in the O 1s region. Thus, re-oxidation and hydroxylation of the surface occurs readily on this chemically active surface.

The C 1s spectra contains a rather broad peak at 284.6 eV, the energy typically assigned to adventitious C found on surfaces exposed to air. This peak showed some intensity on the high binding energy side extending up to about 289 eV, indicating C bound to O in a variety of configurations. As heating progressed, the intensity in this region diminished, leaving primarily hydrocarbons.

3.4. $^{242}PuO_2$

For comparison, a low specific activity (0.003 Ci/g) $^{242}PuO_2$ sample that had been stored in air was studied. The oxide was pressed into Au foil and analyzed in the as-received condition and after heating at 100, 200, 300 and 400 °C. Afterwards, the sample was removed from the vacuum system and exposed to ambient air (in which the relative humidity was approximately 30%) for 15 min and reanalyzed. Fig. 3 shows the Pu 4f and O 1s regions for the $^{242}PuO_2$ sample under these conditions. The second trace from the bottom is for the as-received oxide. The Pu 4f and associated satellite peaks are well defined, suggesting a dominant chemical state with a binding energy for the Pu $4f_{7/2}$ of 427.0 eV, which is higher than the energy expected for stoichiometric PuO_2 (425.5 eV). $Pu(OH)_4$ has a Pu $4f_{7/2}$ binding energy of 426.6 eV, closer to that observed, suggesting extensive hydroxylation of the surface material. The broad O 1s distribution had a peak maximum at 532 eV, where $Pu(OH)_4$ is expected. As the sample is heated to 100 °C, the Pu 4f peaks broaden, with a shoulder emerging at lower binding energies. The O 1s peak similarly changed, with the peak at 529.5 eV becoming more intense – the binding energy assigned to lattice O in PuO_2. Further heating to 400 °C resulted in a stepwise increase of the dioxide peak in the O 1s spectra and well-defined Pu 4f peaks for PuO_2 with a Pu $4f_{7/2}$ peak at 425.5 eV. After 15 min of air exposure, the spectra revert to line shapes and binding energies that resemble those seen after the 100 °C treatment. The increase in this region resembles

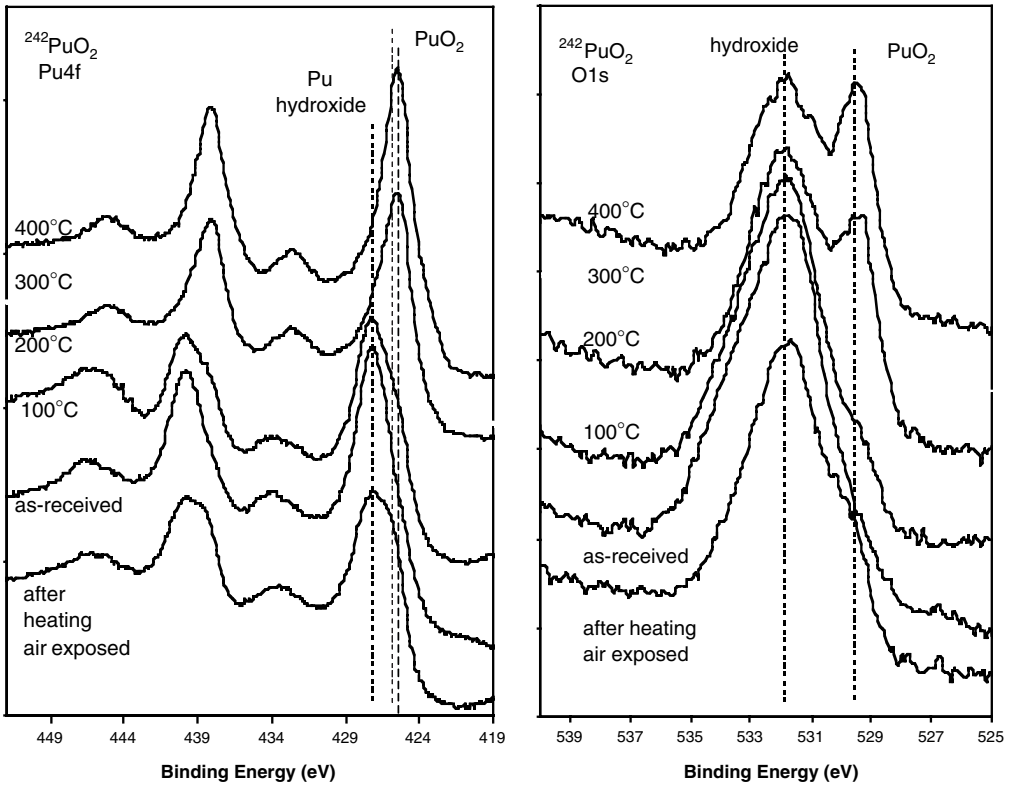

Fig. 3. $^{242}PuO_2$ thermal dehydration. Pu 4f and O 1s regions for a $^{242}PuO_2$ powder sample in the as-received condition, after a series of thermal treatments and after being exposed to ambient air. The Pu 4f peaks shift to lower binding energies and narrow as the surface becomes more like bulk PuO_2. Lattice oxide peaks intensify and grow with respect to the hydroxide region as temperature increases. Upon exposure to air, the surface partially reverts to its original condition.

the adsorption of H_2O and rehydroxylation of the surface that was seen for the heated $^{239}PuO_2$ sample after exposure to 10^{10} L H_2O; but in this case, because the sample was exposed to air, oxy-carbon species were also likely to be involved. The thermally renewed active sites quickly react, nearly reverting to the original as-received condition.

3.5. High specific activity PuO_2

A sample of very high specific activity (7.4 Ci/g) PuO_2 was prepared by pressing the powder into Au foil and analyzed in the as-received condition. Although the dominant isotope is still ^{239}Pu, significant mass fractions of ^{238}Pu (1.9%), ^{240}Pu (26.4%), ^{241}Pu (7.8%) and ^{242}Pu (6.6%) were present. The increased activity of this material was due mainly to the larger mass fraction of ^{241}Pu, which decays primarily by beta emission. However, differences in the surface chemistry (discussed below) are likely due to increased alpha decay from a greater percentage of ^{238}Pu. The near-surface alpha particles with initial energy of 5.5 MeV will produce large numbers of secondary electrons that will excite any adsorbed species, break bonds, and result in a surface more representative of the bulk. The O 1s spectra obtained showed substantially less hydroxide and oxy-carbon and higher intensity for the lattice dioxide peak than those observed for the standard high-fired PuO_2 sample, which had a specific activity of 0.9 Ci/g. The difference in intensities between the lattice dioxide and surface hydroxide peaks was even greater when compared to the $^{242}PuO_2$ sample which had a much lower specific activity of 0.003 Ci/g. The high radiation field apparently has the effect of removing surface contamination, an effect similar to that observed as a result of heating. Fig. 4 shows the Pu 4f and O 1s regions for the high specific activity PuO_2 along with data from the $^{242}PuO_2$ sample after being heated to 400 °C for comparison.

3.6. PuO_{2+x}

A sample of $^{239}PuO_{2+x}$ (described in the experimental section above) was subjected to the same stepwise thermal dehydration treatment as the other oxides. Fig. 5 shows the Pu $4f_{7/2}$ and O 1s regions for the as-received, 100, 200, 300, 400, and 600 °C treatments, from the bottom to the top traces, respectively. The results for this sample differed somewhat from the earlier data collected with the PHI CMA, particularly within the

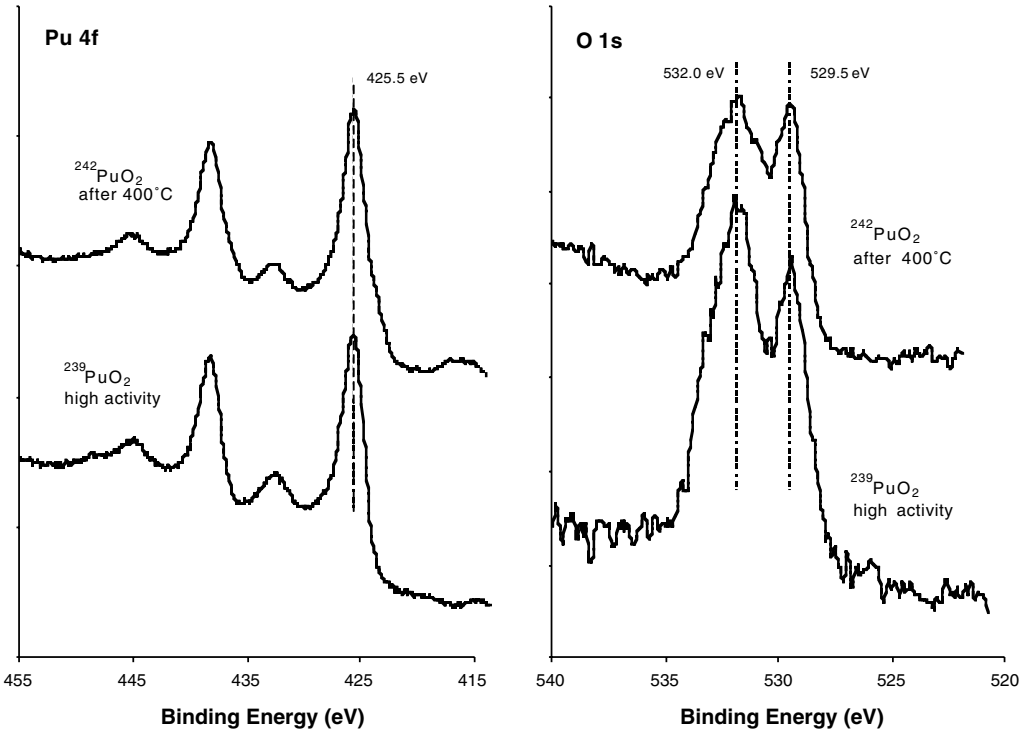

Fig. 4. Thermal vs radiolytic dehydration. Pu 4f and O 1s spectra from the $^{242}PuO_2$ sample after being heated to 400 °C compared to a very high specific activity $^{239}PuO_2$ sample. The spectra are quite similar, suggesting that a high radiation field has the same sort of surface cleaning effect as the thermal treatment.

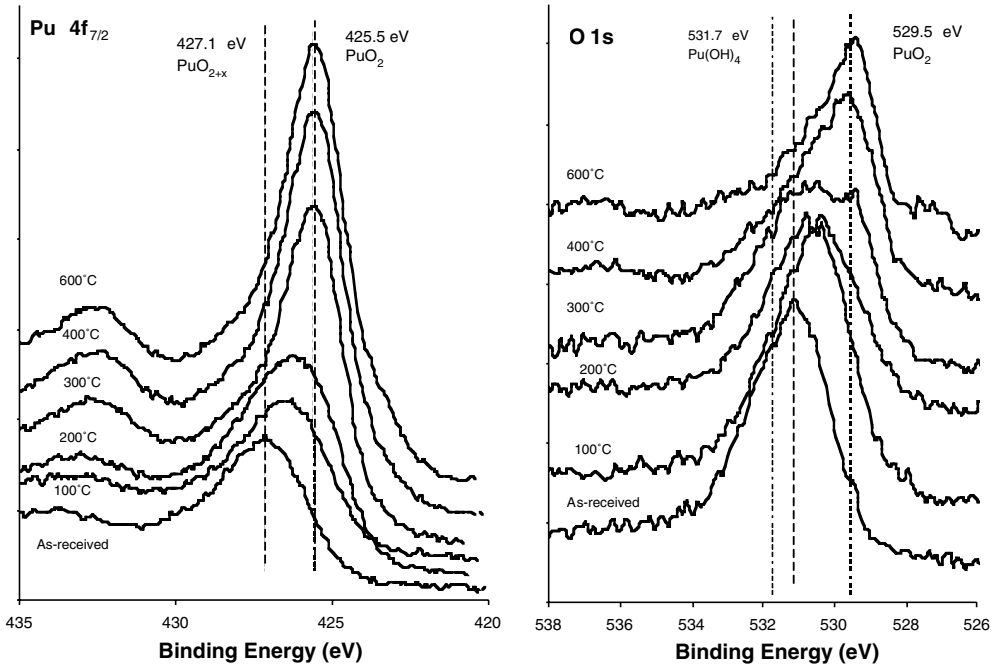

Fig. 5. PuO_{2+x} thermal dehydration. Pu $4f_{7/2}$ and O 1s XPS data collected from the surface of a PuO_{2+x} powder showing spectral changes as the sample was heated to 600 °C. Both peaks show a gradual decrease in binding energy with temperature as H_2O desorbs and hydroxyls decompose, leaving a surface that is more like bulk PuO_2.

O 1s region. In this data set, O 1s binding energies were lower than those seen for the standard high-fired PuO_2 and the $Pu(OH)_4$ sample. The Pu $4f_{7/2}$ binding energy was 427.1 eV, slightly higher than those seen for $Pu(OH)_4$ at 426.8 eV. Spectral features in the Pu 4f region of other PuO_{2+x} samples obtained on the Kratos system were consistent. Some variation in the O 1s region was observed between samples that was likely due to different treatment regimes for this material. Higher O 1s binding energies indicate a greater degree of hydroxylation, which could vary with treatment conditions.

The O 1s region for all of these samples spans the same binding energy range, but the peak centroid for this manifold depends on relative contributions from specific chemical states. As will be described in the curve fitting section below, where the intensities of various bands within the manifold are described.

Pu 4f binding energies for all of the data collected from the PuO_{2+x} samples were consistently high, at about 427 eV, indicating a more electron-withdrawing environment than that of stoichiometric PuO_2. Implications of this higher binding energy are discussed below in the comparison with $Pu(OH)_4$. The thermal dehydration behavior of this material followed the same pattern as the previous two powders with similar changes in binding energies and line shapes with temperature. Differences were observed in the O 1s region due to the dominance of the hydroxyl component vs the greater intensities for the oxy-carbon component for the other dioxides, discussed in the next section on O chemical states. The Pu 4f region shifted to lower binding energy as thermal treatments progressed, finally assumed the characteristics of PuO_2 at the highest temperatures, again showing the effects of surface de-hydroxylation. The gradual shift to lower binding energies for the Pu 4f peaks indicates a change from a more electron-withdrawing hydroxide environment to one that has the spectral features expected for the dioxide. Under the experimental conditions of this study, differences in valence states of Pu can only be resolved by curve fitting, discussed in the section on $Pu(OH)_4$. This sample is most comparable to the $^{239}PuO_2$ sample because they both were heated to about 600 °C and had similar isotopic compositions (similar specific activities). An important difference is that there was no evidence of Pu suboxide formation (peak maximum at 424 eV), perhaps due to the greater availability of lattice O in this sample.

3.7. Oxygen chemical states

The role of surface C is not clear; however, for any samples exposed to air, the broad distribution of chemical states centered around 532 eV includes O bound to C in a variety of forms, as well as hydroxyl groups bound to the Pu. To determine the role of C, its

presence must be controlled – a significant challenge given these powder substrates. Overlapping binding energies confound the analyses as well. Carboxyl bonds have nearly the same O 1s binding energy as surface hydroxyls – about 531.2 eV. The O 1s binding energy for C—O bonds overlaps that for adsorbed H_2O – near 533 eV. These interferences make definite chemical state assignments in the O 1s region above the peak for lattice oxide difficult. Pu bound to both C and O on the surface adds to the intensity observed on the high binding energy side of the Pu $4f_{7/2}$ peak.

Curve fitting was applied to the O 1s regions of selected spectra from the thermal dehydration experiments in an attempt to make chemical state assignments for different bands within the broad envelope. The curve fits for the 100, 200, and 600 °C thermal treatments for PuO_2 and PuO_{2+x} are shown in Fig. 6. The fitted curves are modeled upon the peak shapes and widths that best fit the prominent lattice oxide peaks appearing in the 600 °C spectra. The broad intensity distribution on the high binding energy side of the dioxide peaks can then be fitted with peaks that have the appropriate shape and width for single chemical states. The intensities of these peaks are adjusted to best fit the data. Unless other information is available, conventionally, a minimum number of postulated chemical states (bands) is used to model the raw data. There were at least four chemical states for O on the surface of both samples, because a minimum of four peaks was required to fit the data. It is very likely, however, that other indistinguishable O peaks are part of this manifold. Different chemical states can have similar binding energies that cannot be resolved under these conditions. The only peak that was best fit with a single chemical state assigned to it is the one at 529.5 eV, for lattice dioxide. The other three peaks seen at higher binding energies (about 531, 532 and 533 eV) have less certain assignments. The binding energy values for O as lattice hydroxide have been reported at around 531 eV in a variety of metal hydroxides, including $Mg(OH)_2$ and $Pu(OH)_4$. The rise in intensity that was observed at about 532 eV after 10^{10} L H_2O exposure suggests that adsorbed H_2O and hydroxyl groups in a variety of configurations are implicated in this binding energy range. Adsorbed H_2O typically has the greatest binding energy shift, to about 533 eV.

A closer examination of the distribution of intensities in the three fitted curves shows distinct differences between the PuO_2 and PuO_{2+x} samples, particularly in the spectra measured at 100 and 200 °C. The peak at 532 eV dominates the standard high-fired PuO_2, while the peak at 531 eV is more prominent in PuO_{2+x}. The nature of the process used to produce PuO_{2+x} tends to remove C from the surface, so intensities in the O 1s region due to any C—O bonding are lower. This process also probably

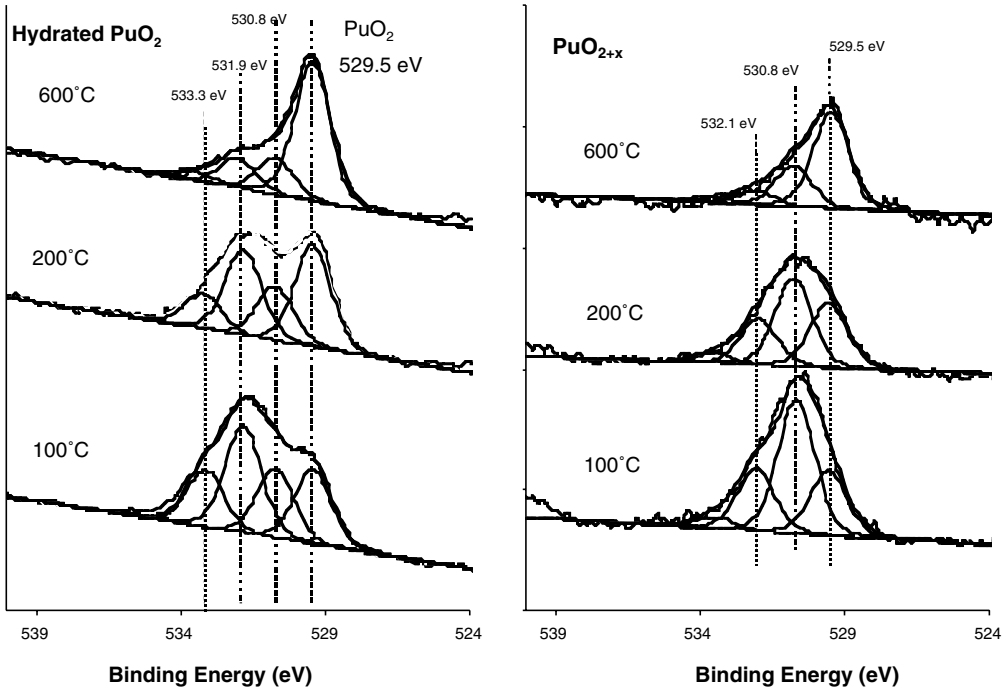

Fig. 6. PuO_2 vs PuO_{2+x} oxygen chemical states. Selected O 1s regions from the thermal dehydration of hydrated PuO_2 compared to the results seen for PuO_{2+x}. The main differences observed were the dominance of the hydroxide feature at about 531 eV for PuO_{2+x} and dominance of C—O bonding (532 eV) for the hydrated PuO_2.

results in extreme surface hydroxylation (compared to 'normal' PuO_2) so the hydroxide peak (531 eV) could be very intense. The PuO_2 sample that was simply exposed to high humidity contains approximately twice as much surface C, a significant fraction of which is in carboxyl bonds, resulting in the intense peak at about 532 eV. The peak at about 533 eV is attributed to adsorbed H_2O and C—O bonds.

3.8. Surface layer thickness estimates

In a storage scenario, gas can be generated by the recombinative desorption of hydroxyl groups to form water which can then be converted to gas. The hydroxylated surface layer thickness of these materials can be used as a rough indication of their gas generation capacity. For the PuO_2 samples exposed at room temperature to H_2O vapor, an escape depth analysis assuming 2.5 nm inelastic mean free path [22] and based on the attenuation and line shape fits of the O 1s spectra estimates that the hydroxylated layer thickness is on the order of 3 nm atop the PuO_2 substrate. This estimate was based on a simple model for these powders that assumes a hydrated layer atop the oxide layer, exponential attenuation of the oxide and hydroxide intensities and a photoelectron take-off angle of 45°. Uncertainties associated with this estimate are mainly due the assumption of a homogenous overlayer and the use of an average take-off angle. Samples with a similar hydroxide to oxide ratio may also have a thicker, but less homogeneous hydroxide-containing layer. Other work [23] suggests that for less than about five monolayers of H_2O (1.0–1.5 nm) hydrogen generation should be negligible Untreated, the hydroxylated surface layers observed for this sample (about 3 nm thick) may cause gas generation problems during storage. The powders will be heated to 950 °C before being sealed in steel containers, thus removing the surface H_2O and decomposing hydroxyls. Exposure to H_2O vapor after heating must be minimized, or the samples will quickly rehydrate, as shown in the section on $^{242}PuO_2$.

3.9. Comparison with $Pu(OH)_4$

Curve fitting data from the $Pu(OH)_4$ powder is shown in Fig. 7, along with a comparison of the curve fits that were done for PuO_2 and PuO_{2+x}. The corresponding Pu $4f_{7/2}$ XPS data in Fig. 7 illustrates the differences observed in the chemical state of Pu in those materials. The Pu $4f_{7/2}$ spectrum for $Pu(OH)_4$ shows a rather narrow peak, indicating a single chemical state. The O 1s region is not as broad as for the other materials, but still encompasses at least three different chemical states. As observed for the oxides, there are significant contributions from hydroxyl groups on the surface in a variety of configurations, as well as surface

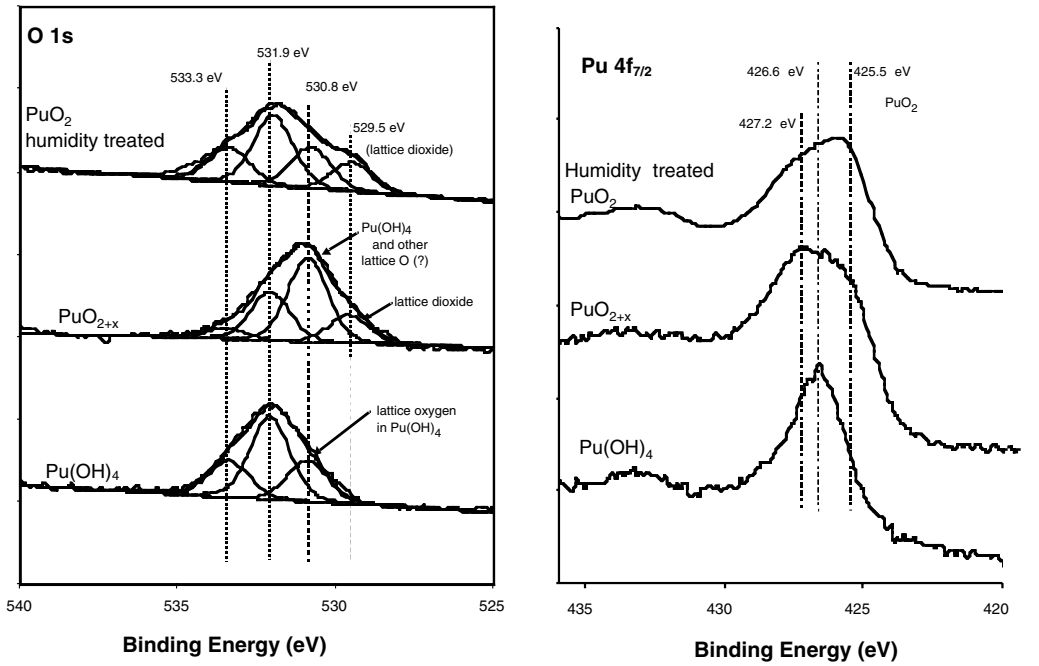

Fig. 7. $Pu(OH)_4$ comparison. O 1s and Pu 4f regions for hydrated PuO_2, PuO_{2+x}, and $Pu(OH)_4$. Differences to note are (1) lack of the lattice oxide feature for $Pu(OH)_4$, (2) greater intensity for C—O bonding for the oxide and hydroxide, and (3) dominance of the hydroxide feature for PuO_{2+x}.

oxy-carbon species. The curve at 530.8 eV is from O bound as lattice hydroxide. Atomic concentration estimates for Pu and O support this conclusion. The atomic ratio for Pu:O based on the total area under the Pu $4f_{7/2}$ peak and the area under the fitted curve at 530.8 eV is about 1:4. Note that there is no intensity for O as dioxide in this spectrum. The fitted curve at 531.9 eV is probably due to a combination of surface hydroxides and oxy-carbon species, and the curve at high binding energy is due to adsorbed H_2O and C—O bonds. As expected, those two peaks (531.9 and 533.3 eV) are less intense in the O 1s region for PuO_{2+x} because of the lower levels of C on that sample.

The most intense peak in the O 1s region for PuO_{2+x} is at 530.8 eV, the peak assigned to lattice hydroxide for $Pu(OH)_4$, and identified as surface hydroxide for PuO_2. This means that the PuO_{2+x} has a surface that is predominantly $Pu(OH)_4$ and/or that O is in another electron-withdrawing environment that causes the same binding energy shift. One possibility is that O is bound to a Pu atom in a higher oxidation state – (V) or (VI) instead of (IV). The rather broad features seen in the Pu $4f_{7/2}$ peaks for both PuO_2 and PuO_{2+x} could encompass several different chemical states: dioxide at 425.5 eV, hydroxide at 426.6 eV and this postulated higher Pu oxidation state at about 427.2 eV. This higher state is more prominent in PuO_{2+x} than in PuO_2, but spectra from both compounds span the same binding energy range and thus may have the same basic components. The asymmetry of the peaks is an indication of the relative amounts of dioxide, hydroxide, and Pu(V) (or Pu(VI)) on the surface and near the surface. Atoms in the lattice can contribute to the intensity, depending on the thickness of the hydroxylated surface layers. The relative intensities of the Pu $4f_{7/2}$ and its associated satellite, which is most prominent for Pu(IV) can be used to estimate the oxidation state purity of the surface material. Intensity ratios of the satellite to the main peak of the PuO_{2+x} were compared to known peak-to-satellite ratios derived from standard high-fired Pu(IV) material. The results indicated that there was about 10% more intensity in the main peak than would be predicted from the satellite. Since the added intensity to the main peak is on the high-binding-energy side (as discussed above) the implication is that some of the Pu is present in a higher oxidation state. Indications of the presence of higher oxidation states in PuO_{2+x} are illustrated in Fig. 8. Differences in the Pu 4f and O 1s core levels between the reacted PuO_{2+x} compared to the unreacted PuO_2 material are: (1) lower intensity of the satellite peaks relative to the main Pu 4f peaks, (2) higher overall binding energy for the Pu 4f lines, and (3) lower overall binding energy for the O 1s region. Observation (1) indicates Pu oxidation states other than +4 are present.

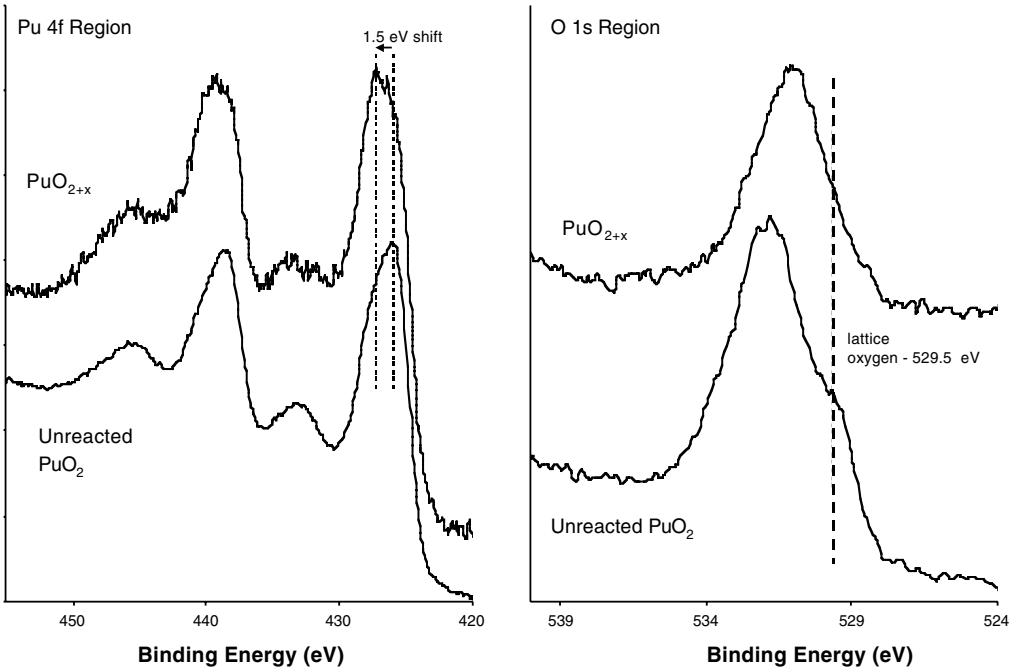

Fig. 8. Core level differences for PuO_2 and PuO_{2+x}. Pu 4f binding energies are shifted about 1.5 eV higher for the PuO_{2+x}, and the satellite intensity is diminished, both suggesting oxidation states greater than +4. O 1s differences can be attributed to a greater degree of hydroxylation for the PuO_{2+x} and more surface C—O bonding for PuO_2.

Observation (2) signifies that these other oxidation states are higher than +4. Observation (3) is due to the preponderance of hydroxyl groups relative to other O-containing species.

XPS results for most Pu oxides show a rather broad distribution of binding energies in the Pu 4f region that would be consistent with different chemical states as well as a smaller fraction (about 10%) of Pu(V) in the mainly Pu(IV) matrix. These results are consistent with the X-ray absorption near edge structure (XANES) and X-ray absorption fine structure (XAFS) work reported by Conradson et al. [24]. A variety of Pu–O distances were observed in that study consistent with the formation of hydroxyls and Pu=O bonds throughout the material as well as on the surface. Some fraction of the Pu was present in the +5 state, so PuO_{2+x} should probably be considered a Pu(IV/V) mixture. The authors also noted a direct relationship between the number of oxo atoms and humidity exposure.

3.10. PuO_2CO_3

Higher oxidation states of Pu can be easily identified by XPS when they are predominant. Fig. 9 shows XPS data from the Pu 4f region for PuO_2CO_3, a Pu(VI) compound in the as-received condition and after decomposing to a Pu(IV) compound. It is likely that exposure to the reducing environment of high vacuum (2×10^{-9} Torr) has had this effect, although no comparison with a control compound was made. The as-received Pu $4f_{7/2}$ binding energy of 428.8 eV and spectral line shape corresponds to what is expected for a Pu(VI) compound. There are no distinct satellites associated with the main peaks. The compound decomposed, as demonstrated by main peaks and shake-up satellites with both energies and relative intensities consistent with Pu(IV) hydroxide. A low intensity shoulder on the high-binding-energy side of the Pu $4f_{7/2}$ peak remains from the original Pu(VI) carbonate. The spectrum of this decomposition product can serve as an example of a mixed valence Pu compound. None of the spectra of oxide and oxyhydroxide samples analyzed in this study displayed such a prominent Pu(VI) oxidation state feature, which suggests that either the Pu(VI) fraction was below the detection limit, or more likely, they are mixtures of Pu(IV) and Pu(V) rather than Pu(IV/VI).

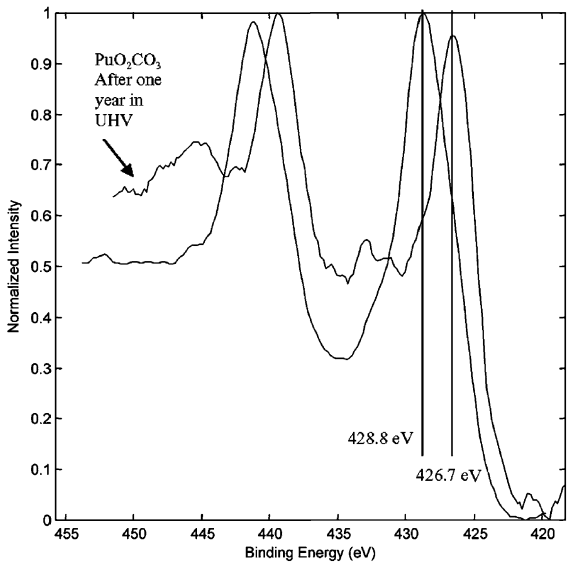

Fig. 9. Pu(VI) to Pu(IV) decomposition. Pu 4f spectra obtained from PuO_2CO_3 showing changes in the surface chemistry after decomposing to a PuIV oxy-hydroxide compound. Peak binding energies shift to lower energies from 428.8 eV for the original Pu(VI) compound to 426.7 eV, and shake-up satellites appear, indicating reduction to Pu(IV).

4. Conclusions

Thermal dehydration experiments of Pu oxides that were prepared and treated under a variety of conditions, coupled with analysis of standard compounds has led to a better understanding of the PuO_2 surface. Surface hydroxylation occurs rapidly at very low H_2O vapor exposure; thus, care must be taken to minimize this exposure of samples intended for long-term storage. At room temperature, the hydroxylated layer can be about 3 nm thick. The surface hydroxides are tenacious and resist thermal decomposition up to 590 °C. Important factors influencing surface chemistry are processing conditions (thermal treatment, in particular) and specific activity. Active sites for the reaction of H_2O and other small molecules can be renewed by thermal energy or by effects of radiation. Other properties such as surface area, particle size and particle morphology, although not specifically addressed in this study, are also expected to be important.

PuO_{2+x} shows evidence of extensive hydroxylation and spectroscopic features that are consistent with higher Pu oxidation states, and suggestive of Pu(V). Curve fitting of the Pu 4f levels indicate that about 10% of the Pu could be in this higher oxidation state. Pu oxide that has been exposed to air will display the complex surface chemistry demonstrated by the hyper-stoichimetric Pu oxide, including a small fraction of oxidation states greater than (IV).

High-fired PuO_2 (heated at 900 °C or higher for hours or longer) has been shown to be more highly ordered and more stoichiometric (purely Pu(IV), thus more difficult to dissolve than low-fired material [25]. The higher degree of surface hydroxylation observed for PuO_{2+x} powders may effectively increase apparent Pu solubility because hydrated PuO_2 ($PuO_2{\cdot}H_2O$ or

$Pu(OH)_4$) has a higher free energy than stoichiometric high-fired PuO_2 and is therefore more soluble and prone to surface corrosion. A review of the solubility of tetravalent actinides found greater solubility for amorphous PuO_2 than for crystalline PuO_2 in acidic solutions [26]. It has been asserted that PuO_{2+x} is both thermodynamically more stable and more soluble than PuO_2 [1]. However, if the solid has a lower free energy, then it will be relatively more stable in the solid state and more stable with respect to dissolution compared with the higher energy compound. Observed increases in solubility could be due to the presence of Pu(IV) colloidal material, which can remain suspended for years, yielding higher apparent solution concentrations. Although inorganic Pu(V) compounds generally have higher solubility products than inorganic Pu(IV) compounds in the same class, the effect that a small fraction of Pu(V) ions in the solid have on overall PuO_2 solubility is not likely to be significant. Any Pu(V) that is solubilized may not remain in that state. Oxidation states of cations in solution are influenced more by solution conditions such as Eh and pH than by their form in the solid [27].

The information presented herein advances the interpretation of XPS spectra for unknown Pu surface species. Pu adsorbed from water on mineral surfaces is often observed by XPS in the +4 state with peak positions and line shapes corresponding to those observed for the humid-air-exposed PuO_2 and $Pu(OH)_4$ samples [28]. The XPS spectra observed on air-exposed Pu metal also share many of the same features – shake-up satellites characteristic of Pu(IV) and broad peaks that indicate multiple chemical states for both Pu and O. Pu 4f binding energies and curve fitting of the O 1s region for these samples has provided a more solid basis for understanding Pu oxide surface chemistry.

Acknowledgements

Pu(IV) colloidal material was provided by Richard G. Haire, Oak Ridge National Laboratory (ORNL). Hyperstoichometric Pu oxide powder with the formula PuO_{2+x} was prepared by Luis Morales, LANL. This research was funded by the Environmental Management Science Program, Office of Biological and Environmental Research, Office of Science of the US Department of Energy and the Los Alamos National Laboratory Directed Research and Development Program.

References

[1] J.M. Haschke, T.H. Allen, L.A. Morales, Science 287 (5451) (2000) 285.
[2] C. Madic, Science 287 (5451) (2000) 243.
[3] USDOE94, Assessment of Plutonium Storage Safety Issues at Department of Energy Facilities. 1994, Department of Energy, Washington, DC.
[4] USDOE00, Stabilization, Packaging and Storage of Plutonium-Bearing Solids, 2000, Department of Energy, Washington, DC.
[5] J.M. Haschke, T.H. Allen, J. Alloys Compds. 336 (1–2) (2002) 124.
[6] D.T. Larson, J. Vac. Sci. Technol. 17 (1) (1980) 55.
[7] R. Baptist et al., J. Phys. F – Metal Phys. 12 (9) (1982) 2103.
[8] D.J. Lam et al., J. Metals 27 (12) (1975) A17.
[9] B.W. Veal et al., Phys. Rev. B – Condens. Matter 15 (6) (1977) 2929.
[10] E. Thibaut et al., J. Am. Chem. Soc. 104 (20) (1982) 5266.
[11] L.E. Cox, J.D. Farr, Phys. Rev. B – Condens. Matter 39 (15) (1989) 11142.
[12] R. Knopp, V. Neck, J. Kim, Radiochim. Acta 86 (3–4) (1999) 101.
[13] M.H. Lloyd, R.G. Haire, Radiochim. Acta 25 (3-4) (1978) 139.
[14] M.H. Lloyd, Nucl. Appl. 5 (1968) 114.
[15] R. Finch et al., Can. Mineral. 37 (1999) 929.
[16] L.A. Morales, Personal communication, 2003.
[17] R.A. Penneman, M.T. Paffett, An Alternative Structure of Pu4O9 (PuO2.25) Incorporating Interstitial Hydroxyl Rather than Oxide, LAUR03-8308, 2003, Los Alamos, NM.
[18] T.W. Newton, D.E. Hobart, P.D. Palmer, Radiochim. Acta 39 (3) (1986) 139.
[19] T.W. Newton, V.L. Rundberg, Mat. Res. Soc. Symp. Proc. 26 (1984).
[20] R.G. Haire, M.H. Lloyd, M.L. Beasley, W.O. Milligan, J. Electron Microsc. 20 (1) (1971) 8.
[21] J.F. Moulder et al., in: J. Chastain, R.C.J. King (Eds.), Handbook of X-ray Photoelectron Spectroscopy, Physical Electronics, Eden Prairie, MN, 1995.
[22] M.P. Seah, W.A. Dench, Surface Interf. Anal. 1 (1) (1979) 2.
[23] M. Paffett et al., J. Nucl. Mater. 322 (1) (2003) 45.
[24] S. Conradson et al., Inorg. Chem. 42 (12) (2003) 3715.
[25] F. Weigel et al., in: J.J. Katz, G.T. Seaborg, L.R. Morss (Eds.), The Chemistry of the Actinide Elements, Vol. 1, 2nd ed., Chapman and Hall, London and New York, 1986.
[26] V. Neck, J. Kim, Radiochim. Acta 89 (1) (2001) 1.
[27] W. Runde et al., Appl. Geochem. 17 (6) (2002) 837.
[28] J.D. Farr, P.K. Schulze, B.D. Honeyman, Radiochim. Acta 88 (9–11) (2000) 675.